

THE TURBULENCE LENGTH SCALES OF SWASH FLOWS GENERATED BY SOLITARY WAVES ON A PLANAR SLOPE

In Mei Sou, Hong Kong Polytechnic University, inmeisou@gmail.com
 Jinghua Wang, Hong Kong Polytechnic University, jinghua.wang@polyu.edu.hk
 Yun-Ta Wu, National Cheng Kung University, ytwu@mail.NCKU.edu.tw
 Philip L.-F. Liu, Cornell University, philiplfliu@gmail.com

INTRODUCTION

Measurements of spatial structures in swash flows are important for development and verification of turbulence models and for the understanding of the fundamental characteristics of turbulence. To accurately calculate the full turbulent energy spatial spectra to examine the energy of the different turbulent energy length scales, the velocity vector field must cover a large spatial extent to include the large-scale energy and must have a fine enough spatial resolution of the order of the Kolmogorov length scale (Pope 2000). This study investigates the turbulent kinetic energy length scales of swash flows generated by six solitary waves on a planar slope in the laboratory. The larger turbulent length scales are resolved with the direct spatial spectrum method using the spatial data obtained by particle image velocimetry (PIV). As the spatial resolution of the velocity field is not fine enough in the PIV measurements, the smaller scales are resolved by the continuous wavelet transform using the temporal data at a fixed-point measurement. We will examine the validity for applying the Taylor frozen hypothesis to the swash flows.

EXPERIMENTS

The spatial velocity data for the six solitary waves on the slope were obtained using PIV measurement technique. The detailed experimental setup and procedure can be found in Wu et al. (2021) and Sou et al. (2023). In this study, we present the turbulent kinetic energy (TKE) spatial spectra during the uprush-downwash interaction between the fourth and fifth solitary waves, during which the flow is at the quasi-steady state.

TKE SPATIAL SPECTRA

The PIV measurements allow direct calculation of turbulent energy spatial spectrum with the velocity field. However, it is not easy to have a large enough area to include the integral length scale and to have a fine enough spatial resolution of the order of the Kolmogorov length scale at the same time. The PIV measurement resolution is $\Delta x = 0.222$ cm and the measurement area is 32.83 cm by 15.17 cm in this study, which is capable of resolving the larger length scale region. As shown in Figure 1, the examples of the spatial spectra indicate that the larger length scales energy region and the spike region corresponding to the energy injection from integral length scales (the large eddies) generated in the swash flow (Figure 1, top panel, $\kappa_1 \langle L_{xx} \rangle \approx 1$). Limited by the relatively large spatial resolution Δx of the velocity field, the dissipation range is not resolved. In addition, the energy injection from the integral length scale generated during the downwash phase modifies the slope in the inertial subrange of the energy cascade from -5/3 to -1 for both TKE spectra $\langle S_{uu} \rangle$ and $\langle S_{ww} \rangle$

(Figure 1, top panel). When the turbulence becomes homogeneous across the x direction during the reversal phase, the typical -5/3 slope for homogeneous turbulence is apparent in the inertial subrange of the energy cascade for both $\langle S_{uu} \rangle$ and $\langle S_{ww} \rangle$ (Figure 1, bottom panel).

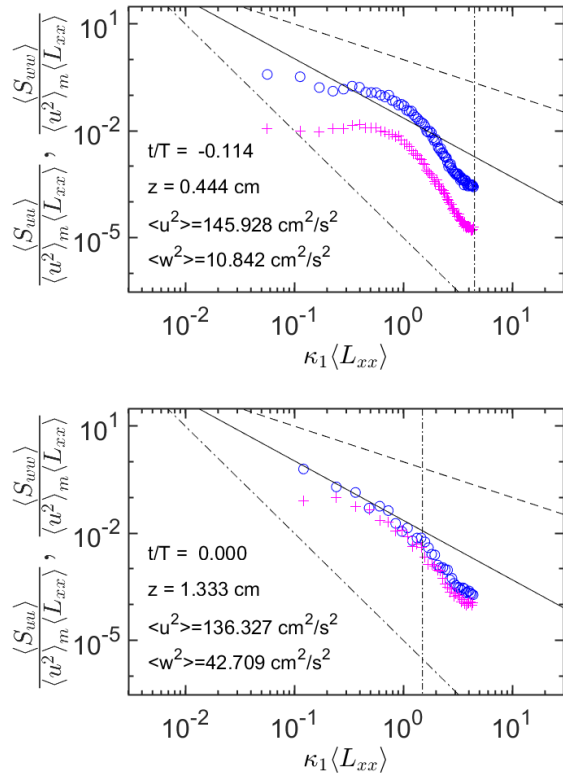


Figure 1 - Examples of the TKE spatial spectra calculated using the PIV spatial data during the downwash phase (top plot) and during the reversal phase (bottom plot). Note that the larger energy scales are shown in the wavenumber spectra (top plot), where κ_1 is the wavenumber in the x direction, $\langle L_{xx} \rangle$ is the integral length scale, $\langle S_{uu} \rangle$ and $\langle S_{ww} \rangle$ are the TKE spectra in the x and w directions, and $\langle u^2 \rangle$ and $\langle w^2 \rangle$ are the variances of the TKE in the x and z directions: $\langle S_{uu} \rangle$ (o); $\langle S_{ww} \rangle$ (+); -5/3 slope (—); -1 slope (-----); -3 slope (-·-·-).

CONTINUOUS WAVELET TRANSFORM

We take advantage of the fast PIV sampling rate of 1000 Hz to resolve the smaller scales in the frequency domain. The continuous wavelet transform is applied to

the turbulent velocity time series of a fixed point to obtain the temporal-frequency spectra (scalogram) so that the smaller scale region can be resolved. The Morlet wavelet is chosen as the mother wavelet of the continuous wavelet transform because the Morlet wavelet resembles the oscillation of the turbulent fluctuation of the swash flows. The mother Morlet wavelet $\psi(t)$ is given by (Torrence & Compo 1998)

$$\psi(t) = e^{i\omega_0 t} e^{-t^2/2} \quad (1)$$

in which ω_0 is frequency and t is time. The analyzing wavelets are generated by wavelet scale a and translation b from the mother Morlet wavelet as

$$\psi_{ab}(t) = \frac{1}{\sqrt{a}} \psi\left(\frac{t-b}{a}\right) \quad (2)$$

where $a > 0, -\infty < b < +\infty$. The continuous wavelet transform of a time series $X(t)$ is defined as the inner product of $\psi(t)$ and $X(t)$ as (Torrence & Compo 1998)

$$W(a, b) = \frac{1}{\sqrt{a}} \int_{-\infty}^{+\infty} X(t) \psi^*\left(\frac{t-b}{a}\right) dt \quad (3)$$

where the asterisk superscript indicates the complex conjugate. By varying the wavelet scale a and the localized time b , a magnitude can be evaluated. In other words, the wavelet transform takes a one-dimensional function of time into a two-dimensional function of time and frequency (or scale).

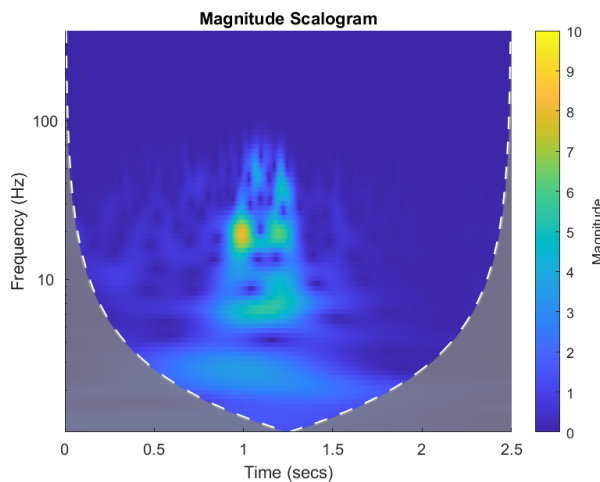


Figure 2 - An example of the TKE scalogram calculated using the continuous wavelet transform with the Morlet wavelet. Note that the smaller energy scales are shown in the temporal-frequency spectra. The time series of the turbulent velocity is at a fixed point $x = -26$ cm and $z = 1$ cm.

An example of the scalogram (Figure 2) shows the temporal evolution of the energy scales from the downwash flow to the uprush flow for the time series at the fixed point $x = -26$ cm and $z = 1$ cm (see Figure 3). The ensemble-averaged vorticity field at a time step for the scalogram is shown in Figure 3, indicating that a

shear layer is formed at this moment during the uprush-downwash interaction. It is apparent that there are several energy spikes in the scalogram (Figure 2), which correspond to the energy injections of different scales generated by the forming of the shear layer. These smaller energy injections are not captured by the spatial spectra shown in Figure 1. The gray area in Figure 2 is the cone of influence. It is caused by the errors that occurred at the beginning and end of the wavelet power spectrum as we are dealing with finite length time series. A vertical slice through the scalogram is a measure of the local frequency spectrum.

We will present the detailed evolution of the turbulence length scales of the uprush-downwash interaction for the swash flows and the validity of the Taylor frozen hypothesis for converting the local frequency spectrum to the corresponding wavenumber spectrum.

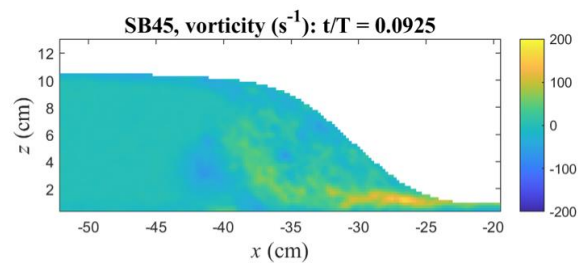


Figure 3 - A time-step snapshot of the vorticity field calculated using the ensemble-averaged velocity field corresponding to the same time series for the TKE scalogram in Figure 2. Note that there is a shear layer during the uprush-downwash interaction at $x = -30$ cm to -24 cm and $z = 1$ cm.

CONCLUDING REMARKS

This study illustrates that it is possible to obtain a large range of energy scales from the spatial spectrum at the fixed measurement point when the sampling rate is fast, and the data record is long. It is beneficial not only for the PIV measurements that we have, but also for other single point measurement techniques, e.g., laser Doppler velocimetry (LDV). It is especially beneficial for examining the field measurement data obtained by the acoustic Doppler velocimetry (ADV) as spatial measurements are difficult to obtain in the field.

REFERENCES

- Pope (2000): Turbulent Flows. Cambridge University Press.
- Sou, Wu, Liu (2023): Swash flows generated by a train of solitary waves on a planar slope, Journal of Fluid Mechanics, vol. 968, A1.
- Torrence, Compo (1998): A practical guide to wavelet analysis, Bulletin of the American Meteorological Society, vol. 79, pp. 61-78.
- Wu, Higuera, Liu (2021): On the evolution and runup of a train of solitary waves on a uniform beach, Coastal Engineering, vol. 170, 104015.